Rothamsted Repository Download

A - Papers appearing in refereed journals

Lowe, R. G. T., Allwood, J. W., Galster, A. M., Urban, M., Daudi, A., Canning, G., Ward, J. L., Beale, M. H. and Hammond-Kosack, K. E. 2010. A combined 1H nuclear magnetic resonance and electrospray ionization-mass spectrometry analysis to understand the basal metabolism of plant-pathogenic Fusarium spp. *Molecular Plant-Microbe Interactions.* 23 (12), pp. 1605-1618.

The publisher's version can be accessed at:

- https://dx.doi.org/10.1094/MPMI-04-10-0092

The output can be accessed at: https://repository.rothamsted.ac.uk/item/8q769/a-combined-1h-nuclear-magnetic-resonance-and-electrospray-ionization-mass-spectrometry-analysis-to-understand-the-basal-metabolism-of-plant-pathogenic-fusarium-spp.

e-**X**tra*

A Combined [1]H Nuclear Magnetic Resonance and Electrospray Ionization–Mass Spectrometry Analysis to Understand the Basal Metabolism of Plant-Pathogenic *Fusarium* spp.

Rohan G. T. Lowe,[1] J. William Allwood,[1] Aimee M. Galster,[2] Martin Urban,[1] Arsalan Daudi,[1] Gail Canning,[1] Jane L. Ward,[2] Michael H. Beale,[2] and Kim E. Hammond-Kosack[1]

[1]Centre for Sustainable Pest and Disease Management, Department of Plant Pathology and Microbiology, Rothamsted Research, West Common, Harpenden, AL5 2JQ, U.K.; [2]The National Centre for Plant and Microbial Metabolomics, Rothamsted Research, West Common, Harpenden, AL5 2JQ, U.K.

Many ascomycete *Fusarium* spp. are plant pathogens that cause disease on both cereal and noncereal hosts. Infection of wheat ears by *Fusarium graminearum* and *F. culmorum* typically results in bleaching and a subsequent reduction in grain yield. Also, a large proportion of the harvested grain can be spoiled when the colonizing *Fusarium* mycelia produce trichothecene mycotoxins, such as deoxynivalenol (DON). In this study, we have explored the intracellular polar metabolome of *Fusarium* spp. in both toxin-producing and nonproducing conditions in vitro. Four *Fusarium* spp., including nine well-characterized wild-type field isolates now used routinely in laboratory experimentation, were explored. A metabolic "triple-fingerprint" was recorded using ^{1}H nuclear magnetic resonance and direct-injection electrospray ionization–mass spectroscopy in both positive- and negative-ionization modes. These combined metabolomic analyses revealed that this technique is sufficient to resolve different wild-type isolates and different growth conditions. Principal components analysis was able to resolve the four species explored—*F. graminearum*, *F. culmorum*, *F. pseudograminearum*, and *F. venenatum*—as well as individual isolate differences from the same species. The external nutritional environment was found to have a far greater influence on the metabolome than the genotype of the organism. Conserved responses to DON-inducing medium were evident and included increased abundance of key compatible solutes, such as glycerol and mannitol. In addition, the concentration of γ-aminobutyric acid was elevated, indicating that the cellular nitrogen status may be affected by growth on DON-inducing medium.

Current address for J. W. Allwood: School of Chemistry, Manchester Interdisciplinary Biocentre, The University of Manchester, 131 Princess Street, Manchester, M1 7DN, U.K.

Current address for A. Daudi: Molecular Plant Sciences, Biological Sciences Department, Bourne Laboratories, Royal Holloway, University of London, Egham, Surrey, TW20 0EX, U.K.

Corresponding author: K. Hammond-Kosack;
E-mail: kim.hammond-kosack@bbsrc.ac.uk

The genus *Fusarium* mainly comprises harmless soil-dwelling saprobes; however, among this group are several economically important agricultural pathogens, including the vascular wilt pathogen *Fusarium oxysporum*; the maize root and stalk rot pathogen *F. verticillioides*; and the causal agent of wheat scab, *F. graminearum*, also known as *Fusarium* ear blight (FEB). FEB is a major problem on wheat, maize, and barley crops (Leonard and Bushnell 2003). FEB results in low-quality grain and the introduction of mycotoxins, such as the sesquiterpenoid trichothecene deoxynivalenol (DON), into the food and feed supply. Control of FEB is limited, with poor genetic resistance provided by commercial cultivars and fungicide application at crop anthesis only partially minimizing DON contamination of the harvest. Currently, the best way to reduce local disease pressure is through rigorous crop residue management combined with a cropping sequence that avoids continuous cultivation of susceptible hosts.

Due to the human and animal health implications associated with the contamination of cereal grain by mycotoxins, considerable efforts have been made to understand the molecular basis for mycotoxin biosynthesis by *Fusarium* spp. The biosynthetic pathway for trichothecene mycotoxin production is well defined and the pathway from primary isoprenoid metabolism to DON has been mapped (Brown et al. 2002; Kimura et al. 2003). The first committed step is the conversion of farnesyl pyrophosphate to trichodiene by the enzyme trichodiene synthase. The next nine steps to synthesize calonectrin are conserved for the synthesis of DON, T-2 toxin, and nivalenol (NIV). Another five reactions are required to convert calonectrin to DON, which can exist in various acetylated forms. Although trichothecene mycotoxins are produced readily during cereal ear infection, during in vitro experimentation they are only produced under specific conditions. These include growth on a nonrepressing nitrogen source, typically either ammonium or agmatine, at a low environmental pH (below pH 4), when high concentrations of simple sugars are available as the carbon source, and when the culture medium is well aerated (Gardiner et al. 2009a and b; Greenhalgh et al. 1986; Miller and Blackwell 1986). The daily addition of hydrogen peroxide has also been reported to increase the accumulation of trichothecenes (Ponts et al. 2009).

Although the production of secondary metabolites has been intensively studied in a range of filamentous fungi, including *Fusarium* spp. (Hestbjerg et al. 2002; Nielsen and Smedsgaard

2003), the primary metabolism of the fusaria has not been addressed as thoroughly. The intracellular metabolite pool of *F. oxysporum* has been profiled during ethanol production in aerobic or anaerobic conditions (Panagiotou et al. 2005c) and a variety of carbon or nitrogen sources (Panagiotou et al. 2005a, b, and d), in a closed bioreactor system. A combination of chromatography and other detection methods were used in these earlier studies in order to capture the range of primary metabolites, and these are the only previous reports on primary metabolism of *Fusarium* spp. The field of metabolomics is well suited to the study of primary metabolism, because it aims to capture as much metabolic information in as nonbiased a manner as possible (Oliver et al. 1998; Teusink et al. 1998). Metabolomics experiments on yeast, based on electrospray ionization–mass spectrometry (ESI-MS) analysis of spent culture medium, have been able to distinguish different growth stages and also differentiate single-gene deletion mutants from the wild-type strain (Allen et al. 2003). A nontargeted ^{1}H nuclear magnetic resonance spectroscopy (^{1}H NMR) and ESI-MS metabolomics approach was chosen as an ideal way to define the biology of *Fusarium* spp. at a metabolic level.

In order to maximize the relevance of this study to the research community, a selection of key species and isolates was chosen for analysis. The four selected species were *F. graminearum*, *F. culmorum*, *F. pseudograminearum*, and *F. venenatum.* In total, nine isolates were included. The *F. graminearum* isolate FgPH-1 of U.S. origin was the isolate most thoroughly investigated in this study (Trail and Common 2000). This isolate is highly pathogenic and produces high levels of the mycotoxins DON, 15-acetyldeoxynivalenol (15-ADON), and zearalenone (Gaffoor et al. 2005). Significant genomic resources are available for this isolate, including full genome sequence information (Cuomo et al. 2007) and a genetic map between FgPH-1 and a second isolate of USA origin Fg00-676 (Gale et al. 2005). Numerous single-gene deletion mutants have already been published in the PH-1 background (Baldwin et al. 2006;

Winnenburg et al. 2006, 2008), and many more have been generated by the community. Further genetic, genomic, and molecular details of the other strains used in this study are presented in Table 1. Isolate Fg16A, collected in Montana, was used to establish a floral pathosystem on *Arabidopsis* for *F. graminearum* (Urban et al. 2002). *F. culmorum* isolate FcUK99 was isolated from the United Kingdom, is fully pathogenic on wheat, and produces DON and 3-acetyldeoxynivalenol (3-ADON) (Dawson et al. 2004). This isolate has been selected for full genomic sequencing (M. Urban, N. Hall, and K. E. Hammond-Kosack, *personal communication*). The two *F. pseudograminearum* isolates, FpCS3096 and FpCS3212 from Australia, are best adapted to infection of the wheat stem base. FpCS3212 is described as moderately aggressive and FpCS3096 as highly aggressive. Both are also fully pathogenic on wheat floral tissue and produce DON and 3-ADON (Akinsanmi et al. 2004, 2006; Li et al. 2008; Mitter et al. 2006). *F. venenatum* FvA3/5 is a soil-dwelling microbe that is nonpathogenic on wheat. This species can produce the trichothecene diacetoxyscirpenol under toxin-inducing conditions but has not been found to produce DON (O'Donnell et al. 1998). Isolate FvA3/5 is currently used as a source of protein for a consumer food (Trinci 1994; Wiebe 2004).

In this study, nine wild-type isolates from four *Fusarium* spp. were analyzed under two liquid-culture growing conditions, mycotoxin inducing and mycotoxin noninducing. These analyses have revealed that the *Fusarium* metabolome is highly flexible and that a triple-fingerprint approach can be used to detect both species and single-isolate differences.

RESULTS

^{1}H NMR of *Fusarium* spp. reveals carbohydrate-rich composition.

We set out to determine whether the ^{1}H NMR method optimized for *Arabidopsis* research, which had not been previously

Table 1. Description of isolates used in the study

Name used	Species	Isolate	Accession	Collection location, and year	Trichothecene chemotype[a]	Additional published information on each isolate
FgPH-1	*Fusarium graminearum*	PH-1	NRRL 31084	Maize grain, Michigan, U.S.A., 1996	15-ADON	10× genome sequence (Cuomo et al. 2007), genetic map with Fg00-676 (Gale et al. 2005), single-gene deletions (Winnenburg et al. 2008)
FgGZ3639	*F. graminearum*	GZ3639	NRRL 29214	Wheat, Kansas, U.S.A., 1990	15-ADON	Genetic map (Bowden and Leslie 1992; Jurgenson et al. 2002), 0.4× genomic sequence (Cuomo et al. 2007)
Fg00-676	*F. graminearum*	00-676	NRRL 34097	Wheat, Minnesota, U.S.A., 2000	15-ADON	Genetic map with PH-1 (Gale et al. 2005)
Fg820	*F. graminearum*	820	Not applicable	Wheat grain, The Netherlands, 1998-99	15-ADON	Transposon mutagenesis study (Luongo et al. 2005)
Fg16A	*F. graminearum*	16A	FGSC8733	Montana, U.S.A., 1997	15-ADON	Genome sequence scan (K. E. Hammond-Kosack, *personal communication*), single-gene deletions (Urban et al. 2002, 2003)
FcUK99	*F. culmorum*	UK99	NRRL 54111	Wheat, Hertfordshire, U.K., 1998	3-ADON	Genomic sequence in progress (M. Urban, N. Hall, and K. E. Hammond-Kosack, *personal communication*) (Baldwin et al. 2010)
FpCS3096	*F. pseudograminearum*	CS3096	CS3096	Wheat crown, New South Wales, Australia, 2001	3-ADON	Wheat crown-rot pathogen, (Akinsanmi et al. 2004; Scott and Chakraborty 2006)
FpCS3212	*F. pseudograminearum*	CS3212	CS3212	Wheat crown, New South Wales, Australia, 2001	3-ADON	Wheat crown-rot pathogen (Akinsanmi et al. 2006)
FvA3/5	*F. venenatum*	A3/5	ATCC PTA-2684	Soil, Buckinghamshire, U.K.	DAS	Nonpathogenic, Quorn food product (Wiebe 2004)

[a] 15- and 3-ADON = 15- and 3-acetyldeoxynivalenol, respectively; DAS = diacetoxyscirpenol.

applied to fungal samples, was adequate for the analysis of *F. graminearum* mycelial extracts (Ward et al. 2003). Polar extracts of *F. graminearum* FgPH-1 mycelia were prepared after 48 h of growth on minimal medium (MM) and ¹H NMR spectrum collected (Fig. 1). In addition, flow-injection ESI-MS in both positive- and negative-ionization mode was performed on the same samples for cross-validation purposes. A typical ¹H NMR spectrum from 9.995 to 0.5 ppm showed a characteristic crowded region from 3.5 to 4.0 ppm, indicating a complex mixture of carbohydrates, including large peaks for sugar alcohols such as glycerol and mannitol, and also for the disaccharide trehalose (Fig. 1B). Signals due to glycine-betaine and choline were among the most intense. Aliphatic amino acids, found in the region from 1 to 4 ppm, were also readily detected, with alanine, leucine, valine, serine, and threonine identified. The acidic amino acids glutamic acid, aspartic acid, and γ-amino butyric acid (GABA) were also identified, along with glutamine, asparagine, proline, methionine, and ornithine. Aromatic amino acids, including phenylalanine, tyrosine, and tryptophan, were identified in the region of 6 to 9 ppm but were generally of lower abundance than the carbohydrates and aliphatic amino acids (Fig. 1C). Some other lower-abundance metabolites were also identified, including adenosine and inosine. When grown solely in MM, *F. graminearum* does not produce the trichothecene mycotoxins DON, 3-ADON, or 15-ADON; therefore, the fingerprint given in Figure 1 represents the combined intracellular and cell-wall-associated metabolome of noninduced *Fusarium* cells.

¹H NMR can be used
to distinguish *Fusarium* spp. and isolates.

Fusarium spp. growing conditions, sample handling procedure, and the ¹H NMR protocol were found to consistently produce good-quality spectra. Therefore, the selected range of *Fusarium* spp. was tested with the aim of determining the metabolic conservation across these various backgrounds. In total, nine *Fusarium* isolates were included in this study. The origins and significance of each are detailed in Table 1. The group comprised five *F. graminearum* isolates, two *F. pseudograminearum* isolates, one *F. culmorum* isolate, and one *F. venenatum* isolate. Their basic growth characteristics were determined in three different ways: after growth on a complete medium (potato dextrose agar [PDA]), by their pathogenicity on wheat ears (Supplementary Fig. S1), and by their production of trichothecenes (Supplementary Fig. S2). Each isolate grew similarly on PDA, with the exception of FvA3/5, which had the slowest growth and a predominantly yellow pigmentation. Because DON was not assayed in early-growth cultures for metabolomics analysis, we independently confirmed by targeted analysis that trichothecenes could be produced under the same conditions when the cultures were grown for longer periods of time. Growth medium from two-stage medium (2SM) cultures was harvested after 25 days in culture and analyzed by gas chromatography–mass spectrometry (GC-MS). *F. graminearum* FgPH-1, Fg00-676, FgGZ3639, Fg16A, and Fg820 produced DON and 15-ADON. *F. culmorum* FcUK99, *F. pseudograminearum* FpCS3096, and FpCS3212 produced DON and 3-ADON. *F. venenatum* FvA3/5 produced diacetoxyscirpenol only. This confirmed that each isolate was capable of producing trichothecenes, and that an extended incubation period in 2SM resulted in accumulation of parts-per-million quantities of trichothecenes. The pathogenicity of all isolates was as expected; Fv A3/5 was nonpathogenic on the susceptible wheat cv. Bobwhite while all others caused significant infection of the inoculated spikelets followed by colonization and bleaching of the remainder of the ear by 14 days post inoculation.

The nine wild-type isolates were grown in MM for 48 h and the mycelium analyzed as before, with the resulting ¹H NMR spectra compared using principal component analysis (PCA) (Fig. 2A and C). Growth rate of isolates was monitored by recording the harvested fresh weight of each culture. Final weights were considered to be roughly equivalent (Supplementary Table 1). Cultures were harvested at 48 h so that the data collected would be representative of the more uniform, rapid-growth phase, rather than from growth-restricted cultures. As culture growth slows, analysis could become complicated by increased cell death, cell lysis, and recycling of released fungal-derived metabolites. The isolates separated into four clearly distinguish-
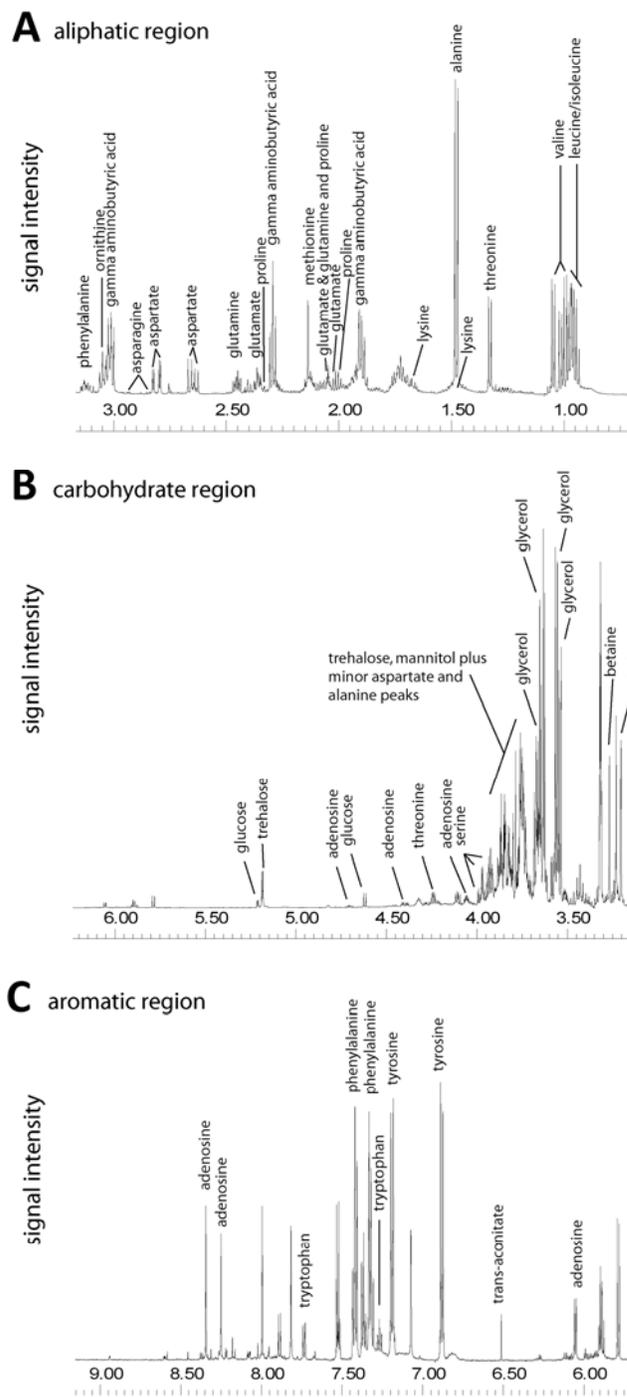
Fig. 1. Representative ¹H nuclear magnetic resonance spectrum derived from *Fusarium graminearum* (PH-1) grown on minimal medium is shown in three sections. Chemical identities of some key metabolites are given. **A,** Aliphatic region; **B,** carbohydrate region; **C,** aromatic region.

able groups: the *F. pseudograminearum* isolates, the *F. venenatum* isolate, and two further groups of *F. graminearum* isolates, one of which included the *F. culmorum* isolate. Principal component one (PC1) included 42% of the variance and resolved the *F. venenatum*, *F. pseudograminearum*, and *F. culmorum* isolates. PC2 (31% of the variance) split the *F. graminearum* and *F. culmorum* isolates from the *F. pseudograminearum* and *F. venenatum* isolates. The PC1 loadings plot was dominated by the signals from sugar alcohols such as mannitol, glycerol, and glycine-betaine (Supplementary Fig. S3).

The F*usarium* metabolome is flexible and highly dependent on the growth medium.

The second growth condition analyzed, 2SM, induced the production of trichothecene mycotoxins. The production of the B-type trichothecene DON is important for FEB disease, and is specifically required for the colonization of the wheat rachis. *F. graminearum* mutants lacking the *TRI5* gene can only infect the local florets within a single spikelet, with progression blocked by cell-wall depositions in the rachis node (Jansen et al. 2005). The comparison of MM (where DON is not produced), with 2SM (where DON is produced) is analo-

gous to the pathogen transiting from early infection in the floret to late infection in the rachis, where DON is required for progression. Compared with MM, 2SM contains higher concentrations of sugars (sucrose at 40 versus 20 g/liter) and has ammonium as the nitrogen source instead of nitrate. In addition, glycerol and sodium chloride were included, all of which slightly decreased the water availability relative to MM. All isolates were grown in 2SM for 48 h and analyzed as before. Because our aim was to define the basal metabolism of the isolates, an intracellular polar metabolome was analyzed to allow comparison with the MM metabolome. The 48-h time point was too early to expect detectable quantities of trichothecenes to be produced; however, the early induction of the *TRI* gene transcription factor *TRI6* would be expected to occur. Therefore, this comparison would focus on shifts in primary metabolism. An overall increase in variation within treatments was observed in the 2SM samples and, therefore, the orthogonal signal correction (OSC) algorithm was applied to remove the most noisy variables prior to PCA (13% of variants were removed). PC1 (53% of variance) generally divided the *F. graminearum* isolates from the other species and also distinguished *F. venenatum* from the two *F.*
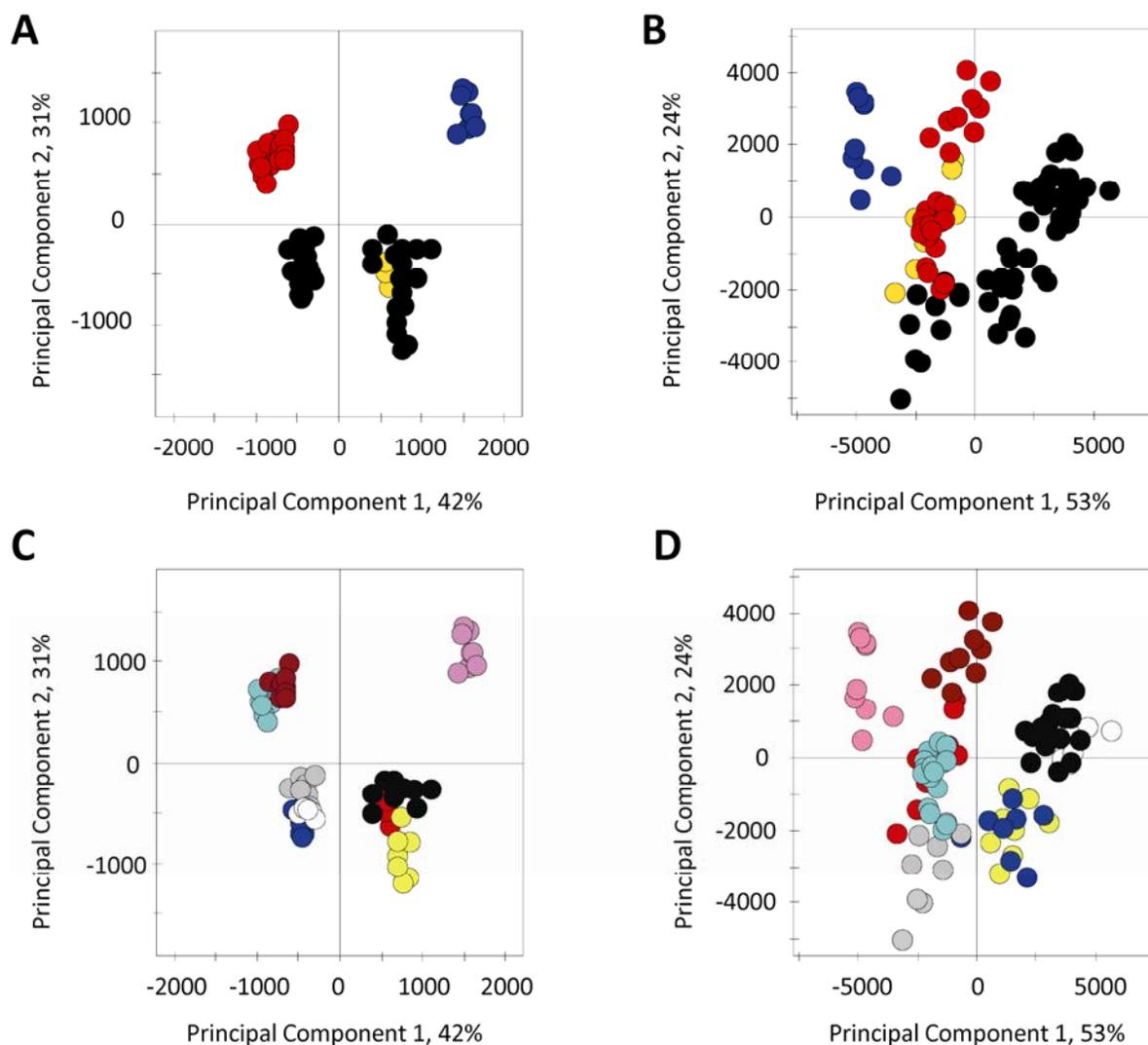
Fig. 2. Growth medium has a large effect on the metabolome of *Fusarium* spp. Principal component analysis (PCA) of ^{1}H nuclear magnetic resonance spectra is shown. Scores plots are given for **A** and **C,** minimal medium cultures and **B** and **D,** two-stage medium cultures. Plots are colored according to **A** and **B,** *Fusarium* sp. (black: *Fusarium graminearum*; yellow: *F. culmorum*; red: *F. pseudograminearum* ; blue: *F. venenatum*) or **C** and **D,** *Fusarium* isolate (black: FgPH-1; red: FcUK99; yellow: Fg16A; blue: Fg820; white: Fg00-676; gray: FgGZ3639; brown: FpCS3212; turquoise: FpCS3096; pink: FvA3/5). Orthogonal signal correction was applied to these datasets prior to PCA.

pseudograminearum isolates (Fig. 2B and D; Supplementary Fig. S4). PC2 (24% of variance) split the *F. graminearum* isolates into three loose groups and clearly resolved the two *F. pseudograminearum* isolates. The remaining 23% of the variance did not present any biologically meaningful separations in the dataset. Unlike in MM, the Fg16A and Fg820 isolates were very similar when grown in mycotoxin-inducing conditions. To determine the effect of the DON-inducing medium on the metabolome, we started by comparing the ^{1}H NMR spectra of FgPH-1 grown on MM with 2SM (Fig. 3). A clear separation was evident in the PCA scores plot (Fig. 3A), with 96% of the variance explained by PC1, which also separated the two media treatments. The loadings plot for PC1 indicated that the aliphatic region of the spectrum between 3.0 and 1.0 ppm contained many differential shifts for the two media (Supplementary Fig. S5). In particular, amino acids were responsible for the difference, including GABA and alanine (Fig. 3B). When all spectra collected from all isolates in both media were combined in a single PCA, this revealed that the isolate differences were smaller than the differences due to growth medium. In the ^{1}H NMR data, all MM samples clustered tightly, while the 2SM samples clustered apart and with more variation (Fig. 4A). PC1 captured 89% of the variance and generally captured the difference between MM samples and 2SM samples. Nine key metabolites were identified that explained the conserved differences between growth conditions (Fig. 4B). These were alanine, glycerol, mannitol, trehalose, betaine, choline, GABA, glutamine, and arginine. In the ESI-MS negative-ion data from the same samples, the ability to distinguish the DON-inducing and noninducing samples was again evident. (Fig. 4C). The loadings plot of PC1 (64% of variance) confirmed some of the key metabolites seen in the ^{1}H NMR data (Fig. 4D). Several of the ions contributing to PC1 could potentially be produced from metabolites that were identified in the ^{1}H NMR spectra; these included m/z 173 [arginine-H]⁻, 181 [mannitol-H]⁻, and 341 [trehalose-H]⁻. The ESI-MS positive-ion data showed a similar trend, with PC1 separating minimal-medium-grown from 2SM-grown samples (Supplementary Fig. S6). Key ions elevated in 2SM-grown samples were m/z 105, 119, 141, 296, 365, and 381. Ions elevated in minimal-medium-grown samples were 145, 167, 176, 258, 318, and 432. Overall, both the ^{1}H NMR and ESI-MS analyses showed that the metabolite differences due to the growth medium were greater than those due to the isolate.

We observed that some of the phylogenetically related isolates grouped apart in one of the media treatments. We compared metabolic fingerprints over the two different media and found that genetically related isolates responded differently to the same growth medium (Fig. 5). For example, the *F. graminearum* isolates FgPH-1, FgGZ3639, and Fg00-676 are more genetically related compared with the isolates from a different species but each produced quite different metabolite spectra after growth in MM. FgPH-1 and FgGZ3639 grown in MM were well separated after PCA of ^{1}H NMR spectra (Fig. 5A). PC1 (79% of variance) accounted for the difference between the two isolates and revealed that FgPH-1 contained higher concentrations of alanine, glutamine, glucose, mannitol, GABA, trehalose, ornithine, and putrescine (Fig. 5C). FgPH-1 and FgGZ3639 isolates were also differentiated by their ESI-MS negative-ion spectra (Fig. 5D). PC1 (77% of variance) contained many discriminatory ions (Fig. 5F), some of which confirmed metabolites identified in the ^{1}H NMR spectra. Ions at m/z 131, 181, and 341 could potentially be produced by ornithine, mannitol, and trehalose, respectively. When FgPH-1 and Fg00-676 were compared after growth in MM, both ^{1}H NMR and ESI-MS negative-ion

spectra produced good separation after PCA (Fig. 5B and E). In the NMR spectra, PC1 (76% of variance) showed that FgPH-1 contained higher concentrations of trehalose and alanine (Fig. 5C). The region between 3 and 4 ppm indicated an abundance of carbohydrates in FgPH-1. The ESI-MS negative-ion data distinguished the two isolates (PC1 contained 85% of the variance), with several ions associated with each isolate (Fig. 5F). The ESI-MS positive-ionization mode data showed a similar separation of FgPH-1 and FgGZ3639 or Fg00-676 samples after growth on MM (Supplementary Fig. S7). Ions elevated in FgGZ3639 versus FgPH-1 were 105, 280, and 296; those reduced were 117, 145, 176, 309, and 318. M/z 280 was the main elevated ion in Fg00-676 samples versus PH-1, while 117, 145, 176, 309, and 318 were reduced. Due to the complexity of adducts produced in negative- and positive-ionization mode, comprehensive identification of all metabolites was not attempted.

The collection of isolates analyzed provides a good range of disease phenotypes, with FgPH-1, Fg00-676, Fg820, FgGZ3639, and Fg16A all causing ear blight disease infecting wheat via the flower at anthesis, while FpCS3096 and FpCS3212 were isolated from crown rot lesions on the wheat
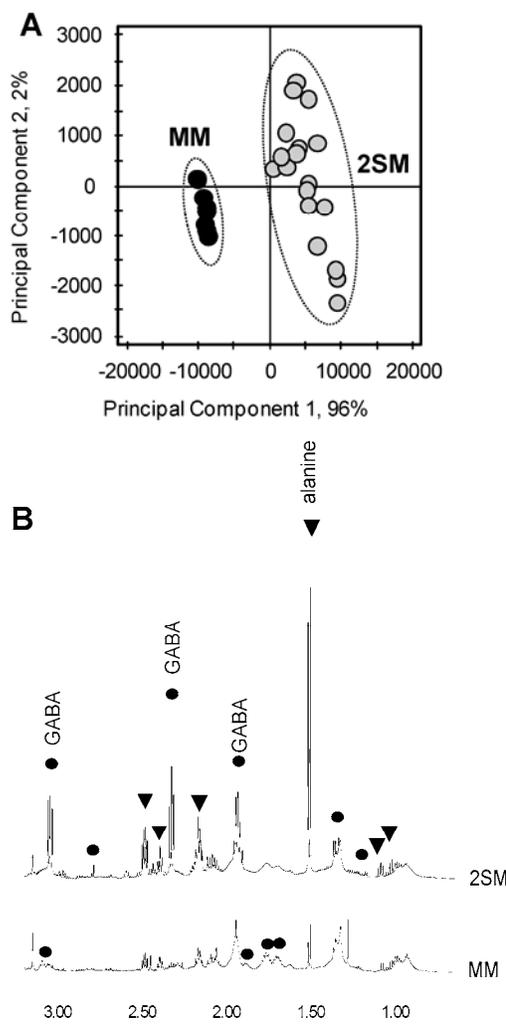
Fig. 3. *Fusarium graminearum* produces certain metabolites in a growth-medium-dependant manner. **A,** Principal component analysis scores plot of ^{1}H nuclear magnetic resonance (NMR) spectra from FgPH-1 grown in two-stage medium (2SM, gray) or minimal medium (MM, black). **B,** Section of the ^{1}H NMR spectrum showing key differences between the two media. Qualitative and quantitative changes are indicated by ● and ▼ symbols, respectively.

stem base. In MM, the low level of nutrients combined with sucrose as the sole carbon source provided a defined environment that mimicked the nutrient found in the wheat apoplastic space. When all isolates grown in MM were compared after PCA, PC2 (31% of the variance) aligned with the difference between all *F. graminearum* ear blight pathogens and the *F. pseudograminearum* crown rot pathogens (Fig. 2C). PC2 loadings indicated that there was a difference in the osmolytes found in each species. *F. graminearum* had higher concentrations of glycerol (3.625 ppm), mannitol (3.855 ppm), and trehalose (5.185 ppm) whereas *F pseudograminearum* was lacking in signals from these metabolites. Instead, this species had several novel shifts in the carbohydrate region between 3.5 and 3.9 ppm, a spectral region where signals for sugar alcohols are located. Additional shifts from amines were found to be stronger in *F. graminearum* isolates, including those for glutamine (2.445

ppm), arginine (1.915 ppm), putrescine (1.765 ppm), and alanine (1.475 ppm).

FvA3/5 is a nonpathogenic soil-dwelling isolate that is unable to cause disease on wheat. FvA3/5 spectra were the most divergent among the minimal-medium-grown samples, scoring highly in both PC1 and PC2 in the PCA. These PCs revealed lower trehalose (5.185 ppm), glycerol (3.625 ppm), and glycine-betaine (3.265 ppm) in FvA3/5 and higher tyrosine (6.875 ppm), phenylalanine (7.325 ppm), and tryptophan (7.525 ppm) in FvA3/5.

The major shifts in metabolism observed when the four *Fusarium* spp. were grown under mycotoxin-inducing conditions (2SM) and mycotoxin-noninducing conditions (MM) were placed into context along with relevant pathway metabolites (Fig. 6). Heat maps depicting the abundance of a total of 28 identified metabolites could be drawn and aligned to the
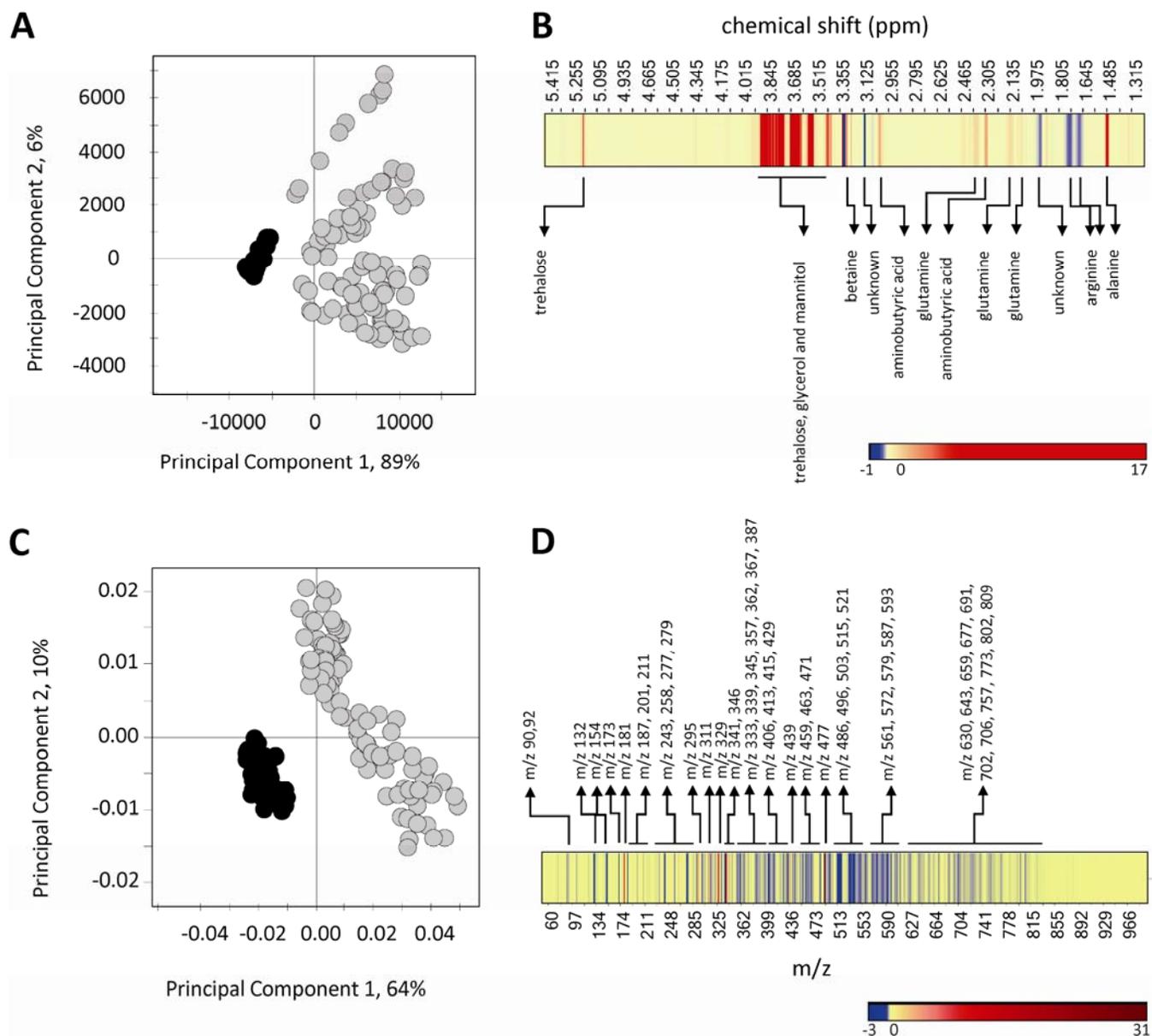
Fig. 4. Changes to the metabolome are conserved across *Fusarium* spp. **A,** Principal component analysis (PCA) scores plot of ^{1}H nuclear magnetic resonance (NMR) data showing differences between all samples grown in minimal medium (MM) (black) and two-stage medium (2SM) (gray); **B,** heat map representation of PC1 contribution plot (from NMR dataset, δ 5.5 to 1.2) illustrating metabolites elevated in 2SM (red) and those which are reduced (blue) relative to MM samples. The aminobutyric acid refers to the gamma form. **C,** PCA scores plot of negative ion electrospray ionization–mass spectrometry (ESI-MS) data showing difference between all samples grown in MM (black) and 2SM (gray); **D,** heat map representation of PC1 contribution plot from ESI-MS dataset illustrating metabolites elevated in 2SM (red) and those which are reduced (blue) relative to MM samples.
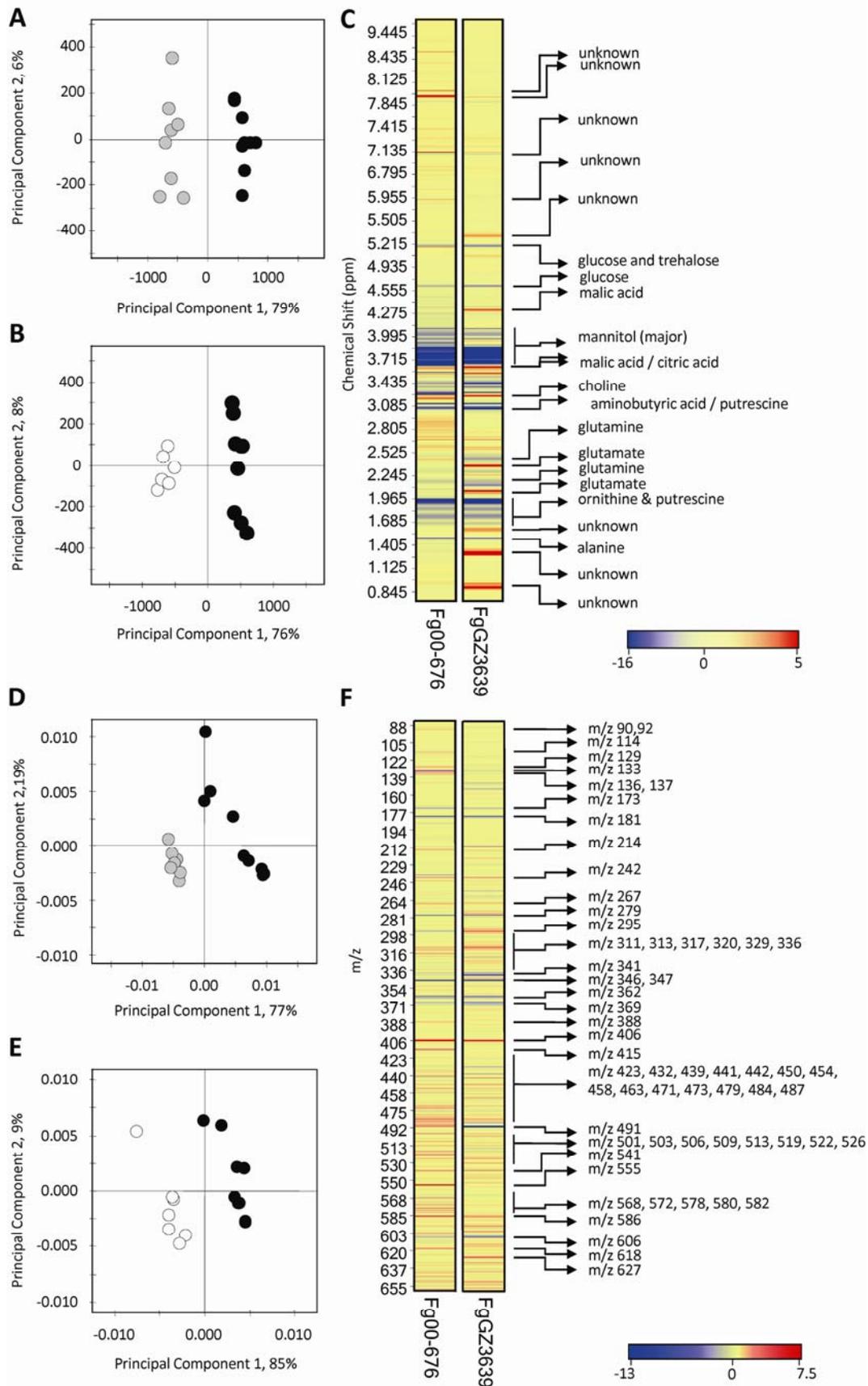
Fig. 5. Isolates from within the same species can be differentiated on the basis of their ¹H nuclear magnetic resonance (NMR) or electrospray ionization–mass spectrometry (ESI-MS) spectra. Principal component analysis of **A,** and **B,** ¹H NMR data of minimal media samples and **C** and **D,** ESI-MS negative-mode data derived from FgPH-1, FgGZ3639, and Fg00-676 (black: FgPH-1; gray: FgGZ3639; white: Fg00-676). For each comparison, a heat map representation of the contribution plot generated from the comparison of isolate to wild type (FgPH-1) is shown. Discriminatory peaks (to FgPH-1) are indicated and annotated (where known). ESI-MS ions are labeled with their nominal m/z value.

Fig. 6. Simplified map of primary metabolism is shown, indicating the relationships between key metabolites identified in this study. Metabolites supplied to cultures directly via growth medium are drawn as a rhombus shape and colored yellow. Characteristic shifts (ppm) of key metabolites confirmed as present in ^{1}H nuclear magnetic resonance (NMR) spectra have relative abundances graphed as a heat-map. The ^{1}H NMR spectral shift used to quantify each metabolite was as follows: alanine (1.475), arginine (1.915), asparagine (2.945), aspartate (2.665), choline (3.205), fructose (4.095), γ-aminobutyric acid (3.005), glucose (4.625), glutamate (2.365), glutamine (2.445), glycerol (3.625), glycine (3.545), glycine-betaine (3.265), isoleucine (1.015), leucine (0.975), mannitol (3.855), methionine (2.145), ornithine (1.945), phenylalanine (7.325), proline (2.015), putrescine (1.765), serine (3.965), threonine (1.335), trehalose (5.185), tryptophan (7.525), tyrosine (6.875), valine (1.055). Metabolites without abundance information were either undetectable or lacked a unique chemical shift. Pathway information was extracted from the Kyoto Encyclopedia of Genes and Genomes (Kanehisa et al. 2008) and drawn using VANTED software (Junker et al. 2006).

Fusarium pathways available from the Kyoto Encyclopedia of Genes and Genomes database.

DISCUSSION

This is the first study which has used combined ^{1}H NMR and ESI-MS analyses of the same material to examine the metabolome of key pathogenic and nonpathogenic *Fusarium* spp. We successfully resolved individual species as well as isolates within a single species on the basis of their metabolome. These data provide a reference baseline to which future experiments in a range of species can be compared. The spectra obtained indicate that the four *Fusarium* spp. contain a consistent set of metabolites, which make up the bulk of the analyzed intracellular metabolome. However, the way this core set of metabolites was regulated was dependant on the isolate. Individual isolates responded to the same stimuli in different manners. The metabolome analyzed either was extracted from the inside of the fungal cells or was still associated with the cell walls after thorough washing. *Fusarium* isolates within a species that had previously been shown to exhibit different disease-causing abilities such as ear blight or crown rot could be readily resolved. The PCA of the ^{1}H NMR and ESI-MS positive- and negative-ionization data was able to resolve the four species explored: *F. graminearum*, *F. culmorum*, *F. pseudograminearum*, and *F. venenatum*. This discrimination at the species level was best achieved when *Fusarium* spp. were grown under non-mycotoxin-inducing conditions (MM). The reduced species or isolate resolution under DON-inducing conditions was most likely due to the requirement for a first-stage culture, which required extra handling and, therefore, could have produced the extra variation between replicate samples. Occasional use of orthogonal signal correction effectively identified and removed noisy variables, while leaving the great majority (87%) of the dataset intact.

Several changes to the *Fusarium* metabolome were detected between growth on the two conditions, across all isolates tested. As mentioned previously, 2SM contains a higher concentration of sucrose, glycerol, and salt compared with MM, and nitrogen is supplied as ammonia rather than nitrate. These differences resulted in elevated concentrations of the compatible solutes glycerol, mannitol, and trehalose in the *Fusarium* intracellular metabolome under the 2SM mycotoxin-inducing conditions. These near-ubiquitous fungal metabolites resist classification into clear cellular roles. Instead, each has been associated with diverse roles such as osmotolerance (de Vries et al. 2003), sporulation (Lowe et al. 2009; Solomon et al. 2006), and regulation of primary metabolism (Wilson et al. 2007). Glycerol was the most abundant metabolite detected in the *Fusarium* polar metabolome, a metabolite most commonly linked to osmotolerance. Ramirez and associates (2006) found that *F. graminearum* isolate RC-22, isolated from wheat in Argentina, produced mannitol as the dominant sugar alcohol during unstressed growth and, as osmotic stress was applied, the predominant species shifted to glycerol (during glycerol-generated osmotic stress) or arabitol (during NaCl stress). Inspection of the growth media used in this study shows that neither contained enough solutes to be considered an osmotic stress medium, which usually contains approximately 1 M glycerol or 1 M NaCl. Possibly, glycerol is simply imported and utilized by *Fusarium* spp. as a compatible solute when available. However, in this study, the most intense signals obtained from the MM-grown samples were still due to glycerol. This result indicates that, in these *Fusarium* isolates, glycerol is synthesized de novo, possibly for a more general role as a compatible solute rather than in response to osmotic stress. Trehalose was detected in all the isolates tested, at various concentrations. *F.*

venenatum A3/5 appears to accumulate trehalose in preference to glycerol in 2SM medium. This could be due to its niche as an exclusively soil-dwelling microbe, whereas the other isolates also attack and reproduce on cereal crops. Trehalose is an osmoprotectant, and generally higher internal concentrations would help *F. venenatum* survive the more varied conditions of the soil. Further work is underway to characterize the response of *F. graminearum* PH-1 to specific environmental stresses applied within our experimental system. The comparison of DON-inducing and MM revealed an increased GABA concentration in all 2SM-grown cultures, and was most evident in FgPH-1 samples. GABA is a key link between the urea cycle and the tricarboxylic acid (TCA) cycle, and can act as part of a TCA cycle bypass around 2-oxoglutarate dehydrogenase. In fungal studies, GABA has been reported to increase in concentration during spore germination in *Neurospora crassa* (Schmit and Brody 1975) and also during citric acid production by *Aspergillus niger* (Kubicek et al. 1979; Kumar et al. 2000). In *A. niger*, the described GABA bypass was due to a TCA block linked to acidogenic conditions; this scenario could be possible in our 2SM cultures because growth on ammonium tends to result in medium acidification in fungi.

It appears that *F. graminearum*, *F. pseudograminearum*, and *F. venenatum* deploy a different set of sugar alcohols and sugars to act as osmolytes during rapid growth. These osmolytes may have been selected for on the basis of their ecological niche in the wheat ear, wheat crown, or soil environment, and could relate to the particular challenges each must overcome to survive in these situations. Furthermore, we found that the ear-blight-causing *F. culmorum* UK99, while genetically distinct from *F. graminearum*, always grouped closely with two other *F. graminearum* isolates (O'Donnell et al. 2004). A more systematic survey of isolates from the full range of *Fusarium* ecological niches may provide a clearer indication of the relationship between osmolytes and the pathogen environment.

The resolution obtained by all three technologies was sufficient to distinguish between isolates within the species *F. graminearum* and *F. pseudograminearum*. This fine degree of resolution was unexpected. NMR is generally not as sensitive a technique as MS methods, and it was thought that within-species differences would be difficult to detect in the ^{1}H NMR datasets. This was shown to be incorrect because several isolates from the same species were resolved by ^{1}H NMR under either of the two culture conditions. The isolate differences detected altered according to the growth medium used, and demonstrated the plasticity of the metabolome and the ability of fungi to alter their intracellular content dramatically in response to the external environment. An interesting aspect of the data is that differences between the *F. graminearum* isolates could not be explained by geographical origins. Four *F. graminearum* isolates came from the United States, while one (Fg820) came from The Netherlands. The Fg820 isolate was indistinguishable in the PCA from Fg00-676 in MM and Fg16A in 2SM. This could be interpreted to mean that geographical location cannot be used to predict metabolic relatedness, perhaps due to metabolic plasticity or rapid spread of isolates around the globe. We were able to identify the key metabolic differences between FgPH-1, the model cereal-infecting *Fusarium* isolate, and FgGZ3639 or Fg00-676. These three isolates have been assigned to *F. graminearum* (formerly genetic lineage 7) on the basis of sequence diversity in 11 nuclear genes (O'Donnell et al. 2004).

The level of resolution of closely related *Fusarium* isolates means that there is the potential to combine existing genetic mapping populations available for *F. graminearum* with metabolic fingerprints observable with ^{1}H NMR and ESI-MS. PH-1 and 00-676 are the parents for a genetic map created by Gale

and associates (2005) and are resolvable when compared after growth in either condition tested here; an analysis of additional growth conditions would undoubtedly increase the number of traits. Phenotyping via metabolomic fingerprinting would be particularly beneficial when trying to map and then identify the genes required, directly or indirectly, for the production of novel metabolites. Such an approach has been successfully used in the analysis of wheat- and tomato-mapping populations (Hamzehzarghani et al. 2005; Schauer et al. 2006), and could easily extend to existing fungal-mapping populations.

Metabolic fingerprinting is ideal for classifying isolates, because it can quickly provide phenotypic data that can be used to compare relatedness, with little prior knowledge required about the isolates (Kouskoumvekaki et al. 2008). Direct-injection ESI-MS has been successfully used to classify *Penicillium* spp. and isolates (Smedsgaard and Frisvad 1996, 1997; Smedsgaard and Nielsen 2004). Use of a single growth medium and direct-injection ESI-MS was sufficient to assign correctly 70% of isolates into their species group, as previously determined using a polyphasic approach including growth characteristics (Frisvad and Samson 2004). The use of metabolomic fingerprinting in MM, the most discriminatory condition tested, could be used to compare isolates that show a wide range of DON mycotoxin-producing abilities or virulence toward wheat. Starkey and associates (2007) described a global collection of 2,100 FEB isolates, including new species of *Fusarium* and some isolates with chemotypes not previously found in their geographical region. This population was organized into a defined phylogeny and could be sampled in order to capture the maximum metabolic variance in the *F. graminearum* species complex. Alternatively, Ward and associates (2008) reported the recent emergence in North America of a highly toxigenic and genetically divergent population of 3-ADON-producing *F. graminearum*. In this case, metabolic fingerprinting by ^{1}H NMR and ESI-MS could rapidly add further layers of phenotypic information to these novel populations, perhaps revealing the underlying basis for their selective advantage.

In this study, positive identification of any of the known toxins or secondary metabolites made by *Fusarium* spp. in our ^{1}H NMR or ESI-MS spectra was not possible. Although ^{1}H NMR is an ideal technique for metabolic fingerprinting, it is not as sensitive as MS techniques. Therefore, it is not surprising that secondary metabolites were not identified in our ^{1}H NMR spectra. Also, because both conditions tested involved short incubation times (48 h), secondary metabolites would be at an early phase of accumulation. Indeed, the predicted ions for 15-ADON and 3-ADON were not found in the more sensitive ESI-MS spectra for 2SM samples. The metabolic fingerprint during stationary phase growth would have been far more challenging to study because, by this stage, a large proportion of the culture is already undergoing cell death. The 48-h time point was selected for this baseline fingerprinting analysis because, at this stage, *Fusarium* spp. growth is rapid and the mycelium of each isolate is of a relatively homogenous composition. In addition, the trichothecene mycotoxins are secreted into the extracellular environment, whereas we analyzed the mycelium for metabolomics analysis. The mycelium-only sample increases the difficulty in detecting mycotoxins at an early time point. To help clarify the situation, we used a trichothecene-specific GC-MS technique to analyze trichothecene content in the two growth media after longer culture periods. This confirmed that all nine isolates were competent to produce known trichothecenes in parts-per-million quantities under the conditions selected after 25 days. This is much later than the time point used for the metabolomics analysis. The targeted analyses also revealed that DON was produced at approximately $^{1}/_{10}$ the concentration of either acetylated form, and the alterna-

tive acetylated DON at approximately 5% of the predominant form. The concentrations of the alternative DON chemotype are very low and were expected, given the sensitivity of the assay method and the extended period of growth in 2SM. During DON biosynthesis, a double-acetylated intermediate (3,15-ADON) is first made and then selectively deacetylated by the TRI8 enzyme to produce either 3-ADON or 15-ADON, depending on the *TRI8* genotype (Alexander et al. 2010). The small amounts of 3-ADON identified in the 15-ADON chemotype were probably due to either nonspecific enzymatic activity or an unknown breakdown mechanism in the culture medium.

The era of systems biology and high-throughput techniques that generate large nontargeted datasets has opened the way for the construction of cellular simulations. By combining information from whole-genome sequencing (Cuomo et al. 2007), gene expression profiling (Guldener et al. 2006), proteomics (Taylor et al. 2008), and conserved biochemical pathways (Kanehisa et al. 2008), it is possible to predict a set of pathways present in a particular organism (Forster et al. 2003; Herrgard et al. 2008). Now, data for a range of metabolites can be included for several *Fusarium* spp. Once a simulation of the cell's metabolism is constructed, the effects of single-gene deletions or other perturbations could be predicted with more certainty. Also, simulations can be used to highlight aspects of cellular metabolism that may be missed by current analyses. Ideally, these types of studies could be used to identify aspects that are critical to pathogenic growth or toxin production, which could subsequently be targeted to develop novel disease control strategies. Through the collection of nonbiased high-quality data, these simulations will, over time, become increasingly representative of the true biological situation. Toward this end, we have placed the main metabolites consistently identified as regulated under mycotoxin-inducing and mycotoxin-noninducing conditions in this baseline study into a pathway map (Fig. 6). These key metabolites include several carbohydrates often associated with fungi—trehalose, mannitol, and glycerol—as well as the nitrogen-containing metabolites alanine, choline, betaine, GABA, glutamic acid, and glutamine. The identification of choline and betaine in *Fusarium* spp. is of note because these amines are found in wheat anthers and have been shown to have a growth stimulation effect on *F. graminearum* (Strange and Smith 1978; Strange et al. 1974). It will be useful to determine whether they are imported and metabolized during infection or whether the stimulation effect is transduced via extracellular receptors.

Thus far, the use of metabolomic fingerprinting has been reported for a handful of plant pathogens interacting with their hosts (Allwood et al. 2008). These include the rice blast fungus *Magnaporthe oryzae* on the model plant *Brachypodium distachyon*, *Oryza sativa*, and *Hordeum vulgare* (Allwood et al. 2006; Parker et al. 2009); the leaf-blotch fungus *Mycosphaerella graminicola* on wheat (Keon et al. 2007); the bacterial wilt pathogen *Pseudomonas syringae* on tomato (Rico and Preston 2008); phytoplasma-infected *Catharanthus rosea* (Choi et al. 2004); and *Tobacco mosaic virus*-infected *Nicotiana tabacum* (Choi et al. 2006). These studies are usually limited by the difficulty in distinguishing host from pathogen metabolism, and focus on the host response. The largely conserved response to medium composition shown by the isolates in this study suggests that the external environment is critical to determining the internal metabolite profile of these pathogens. We also know that mycotoxin synthesis is highly influenced by the external growth environment. These observations suggest that, if cereal hosts could be manipulated to accumulate metabolites known to inhibit mycotoxin synthesis, they may be effective against a broad spectrum of *Fusarium* spp. With a similar aim, Browne and Brindle (2007) combined FEB

latent period data and ^{1}H NMR spectra from a collection of the Centro Internacional de Mejoramiento de Maíz y Trigo wheat genotypes. They predicted the latent period of each genotype based on ^{1}H NMR spectra, and found a significant correlation between their predicted latent periods and experimentally verified values. Some of the metabolites with the most influence on latent period (choline, betaine, alanine, glutamine, and glutamate) were also identified in our study as abundant in *Fusarium* isolates. Ideally, the concentration of these key wheat metabolites should be manipulated in an isogenic background to see if they directly influence resistance to FEB or are simply linked to the presence of a FEB resistance locus.

For this study, a metabolomics protocol originally developed for the analysis of *Arabidopsis thaliana* (Ward et al. 2003) was successfully used to explore the intracellular metabolome of *Fusarium* spp. This study has revealed that the metabolome of the model *F. graminearum* PH-1, for which considerable genomic sequence information is available, is centrally placed among the four *Fusarium* spp. and the eight isolates originally selected because of their own experimental importance. Although this was a purely in vitro study, successful identification of the numerous *Fusarium* spp.-produced metabolites identified by a triple-fingerprint approach will be invaluable when considering the various in planta interactions.

MATERIALS AND METHODS

Cultures and growth conditions.

Cultures used were *F. graminearum* FgPH-1 (FGSC 9075; Fungal Genetics Stock Center, Kansas City, MO, U.S.A.), Fg16A (FGSC 8733; L. Lahman, Monsanto, St. Louis), Fg820 (C. Waalwijk, Wageningen University, The Netherlands), GZ3639 (NRRL 29214), Fg00-676 (NRRL 34097), *F. culmorum* FcUK99 (FGSC 10436; G. Bateman, Rothamsted Research, Hertfordshire, U.K.), *F. pseudograminearum* FpCS3096, FpCS3212 (J. Manners, CSIRO, Brisbane, Australia), and *F. venenatum* FvA3/5 (G. Robson, British Mycological Society, Manchester, U.K.). More information on each of these isolates is presented in Table 1.

All isolates were routinely subcultured on synthetic nutrient-poor (SN) medium, consisting of KH_2PO_4 at 1 g/liter, KNO_3 at 1 g/liter, $MgSO_4 \cdot 7H_2O$ at 1 g/liter, KCl at 0.5 g/liter, glucose at 0.2 g/liter, and sucrose at 0.2 g/liter, with agar at 20 g/liter added for solid media. Cultures were incubated at 25°C under a combination of white light and near-UV light. Conidia were harvested from a mung-bean liquid culture as described by Bai and Shearer (1996), and 100 ml of mung bean extract was inoculated with a mycelial plug and incubated at 28°C for 4 days with shaking. Conidia were separated from the mycelium by filtration though Miracloth (Calbiotech, La Jolla, CA, U.S.A.), washed three times in sterile water, and stored at 4°C for less than 1 week prior to use.

For metabolomics analysis, liquid broth (100 ml) was inoculated to 1×10^4 conidia/ml and incubated in 250-ml flasks at 22°C and 100 rpm for 2 days in the absence of light, except for *F. venenatum* FvA3/5 cultures, which were inoculated to mycelium at 1 mg/ml derived from a potato dextrose broth (Formedium, Norfolk, U.K.) culture. Metabolomic cultures were made in either MM broth or trichothecene-inducing medium. MM consisted of KH_2PO_4 at 1 g/liter, KNO_3 at 1 g/liter, $MgSO_4 \cdot 7 H_2O$ at 1 g/liter, KCl at 0.5 g/liter, sucrose at 20 g/liter, and glucose at 0.2 g/liter. The trichothecene-inducing medium devised by Harris and associates (2007) was done as originally described but with some modifications. Conidia were harvested from mung bean broth cultures and used to inoculate 100 ml of 1SM broth (NH$_4$Cl 3 g/liter, MgSO$_2 \cdot$ 7H$_2$O at 2 g/liter, FeSO$_4 \cdot$ 7H$_2$O at 0.2 g/liter, KH$_2$PO$_4$ at 2

g/liter, peptone at 2 g/liter, yeast extract at 2 g/liter, malt extract at 2 g/liter, and glucose at 20 g/liter) to 1×10^4 conidia/ml, and incubated at 22°C and 100 rpm for 2 days. The mycelium was then harvested by vacuum filtration, washed in sterile water, and transferred to a new flask of 100 ml of 2SM broth ((NH_4)$_2$HPO$_4$ at 1 g/liter, KH_2PO_4 at 3 g/liter, $MgSO_4 \cdot 7H_2O$ at 0.2 g/liter, NaCl at 5 g/liter, sucrose at 40 g/liter, and glycerol at 10 g/liter) and incubated at 22°C and 100 rpm for a further 2 days prior to harvest.

Metabolite extraction.

Mycelia were harvested by vacuum filtration, washed three times in distilled water, and snap frozen under liquid nitrogen. Metabolite extraction and analysis methodology was based on that described previously (Ward et al. 2003, 2010). Ground freeze-dried material (15 mg) was resuspended in 1 ml of 80:20 $D_2O:CD_3OD$ containing 0.05% (wt/vol) d$_4$ TSP (sodium salt of trimethylsilylpropionic acid) and then heated at 50°C for 10 min. After cooling, the samples were spun down in a microcentrifuge for 5 min. An 850-μl aliquot of the supernatant was then heated at 90°C for 2 min, cooled to 4°C for 45 min, and recentrifuged for 5 min. A 750-μl aliquot of the supernatant was added to a 5-mm NMR tube for ^{1}H NMR, while another 50-μl aliquot was mixed with 950 μl of 80:20 $D_2O:CD_3OD$ for parallel ESI-MS analysis.

Data collection.

All ^{1}H NMR spectra were acquired under automation at a temperature of 300 K on a Bruker Avance spectrometer operating at 600 MHz ^{1}H observation frequency using the SEI 5-mm probe. The WATERSUP pulse sequence was used with a relaxation delay of 5 s. Each spectrum consisted of 128 scans of 64,000 data points. The spectra were automatically Fourier transformed using an exponential window with a line broadening value of 0.5 Hz, then phased and baseline corrected within the automation software. ^{1}H NMR chemical shifts in the spectra were referenced to d$_4$ TSP at δ 0.00. ESI-MS data was collected on a Bruker Esquire 3000 mass spectrometer.

Data reduction of spectra.

The ^{1}H NMR spectra were automatically reduced to ASCII files using AMIX (Analysis of Mixtures software v.3.0; Bruker Biospin, Billerica, MA, U.S.A.). Spectra were scaled to d$_4$ TSP and reduced to integrated regions or "buckets" of equal width (0.01 ppm) corresponding to the region of δ 9.995 to δ –0.5. The regions between δ 4.865 and δ 4.775 were removed prior to statistical analyses, thus eliminating any variability in suppression of the water signal. The signals corresponding to d$_4$ methanol (δ 3.335 - δ 3.285) and d$_4$ TSP (δ 0.00) were also removed at this stage. The ASCII file was imported into Microsoft Excel for the addition of labels and then imported into SIMCA-P 11 (Umetrics, Umea, Sweden) for multivariate analysis. All data was mean-center scaled. PCA was carried out on all data sets.

GC-MS for trichothecenes analysis.

Trichothecene mycotoxins were analyzed by GC-MS, with a protocol derived from that published by Tacke and Casper (1996). Used culture medium (630 μl) was added to 3.37 ml of acetonitrile (Fisher Scientific, Waltham, MA, U.S.A.) and 1.3 μg of DOM-1 internal standard (Biopure, Tullin, Austria) in 1 ml of acetonitrile, vortexed briefly, and extracted for 60 min at room temperature. The entire solution was then passed though an SPE cleanup column. SPE columns (8 ml) contained 1 g of packing material, consisting of a 1:3 ratio (wt/wt) of C18 sorbent (Grace Davison, Columbia, MD, U.S.A.) and Al_2O_3 (Sigma Aldrich, St. Louis). Column eluate (1 ml) was then

evaporated to dryness under vacuum and then derivatized with 100 μl of 100:1 TMSI:TMCS (Pierce, Rockford, IL, U.S.A.) for 15 min at room temperature. The derivatized sample was added to 1 ml of iso-octane and 1 ml of milli-Q purified water, vortexed for 15 s, and the upper organic phase analyzed by GC-MS. A 2-μl aliquot was analyzed (splitless injection) using a Hewlett-Packard 5890 gas chromatograph and a Hewlett-Packard 5970 Series mass selective detector (Agilent, S. Queensferry, West Lothian, U.K.) using a 30-m Zebron Guardian ZB-5 column. Mass spectra were acquired in scan mode and selected ion monitoring (SIM) mode over 40 to 650 m/z from 6.00 to 20.00 min with a dwell time of 50 milliseconds. The GC injector and transfer line were both held at 250°C. Helium was used as the carrier gas. The oven temperature was kept at 70°C for 2 min and ramped to 350°C at 17°C min^{-1}, with a further hold at this temperature for 1.5 min. Data were quantified using MassLynx 4.0 (Waters, Manchester, U.K.). Trichothecene calibration curves for authentic DON, 3-ADON, 15-ADON, and NIV (Biopure) were constructed to span 0.05 to 25 μg/ml. Quantification of trichothecenes was performed on extracted ion traces. Peak areas were calculated relative to the area of the DOM-1 internal standard. The extracted ions were DOM-1 (11.06 min), m/z 391; DON (11.66 min), m/z 235; 3-ADON (12.19 min), m/z 193; 15-ADON (12.26 min), m/z 193; and NIV (12.28 min), m/z 289.

Pathogenicity assays on wheat.

Pathogenicity assays on wheat ears of the highly susceptible spring cv. Bobwhite were done using the point inoculation method, by placing a 10-μl conidia suspension (10^{-4} conidia/ml) into each of the middle two spikelets when the ear was at 30% anthesis. Plant growth, incubation conditions, and disease assessment regimes were the same as described previously (Urban et al. 2002, 2003). A minimum of three ears were inoculated per isolate.

Experimental replication and statistical analyses.

Liquid cultures were grown in triplicate with three technical replicates for analysis prepared per sample. The occasional serious outlier was identified and removed from datasets prior to analysis. All statistical analyses were performed with SIMCA-P software (Umetrics, Umeå, Sweden), including analysis of variance, PCA, and partial least squares. All data was mean-center scaled during PCA. If required, OSC was applied within SIMCA-P software to datasets to identify and remove noisy variables that were noninformative in relation to treatment groupings (Wold et al. 1998). These instances are noted in the relevant figure legend or main text.

Primary data.

Complete data tables for the ^{1}H NMR , ESI-MS negative-ion, and ESI-MS positive-ion experiments are provided in Supplementary Tables 2 through 4. For ^{1}H NMR data, the spectra bucket tables derived from the original spectra are presented. These datasets are composed of raw values, prior to orthogonal signal correction.

LITERATURE CITED

Akinsanmi, O. A., Mitter, V., Simpfendorfer, S., Backhouse, D., and Chakraborty, S. 2004. Identity and pathogenicity of *Fusarium* spp. isolated from wheat fields in Queensland and northern New South Wales. Aust. J. Agric. Res. 55:97-107.

Akinsanmi, O. A., Backhouse, D., Simpfendorfer, S., and Chakraborty, S. 2006. Pathogenic variation of *Fusarium* isolates associated with head blight of wheat in Australia. J. Phytopathol. 154:513-521.

Alexander, N. J., McCormick, S., Waalwijk, C., and Proctor, R. H. 2010. Genetic basis for the 3ADON and 15ADON trichothecene chemotypes in *Fusarium graminearum*. In: 10th Eur. Conf. Fungal Genetics, Leiden, The Netherlands.

Allen, J., Davey, H. M., Broadhurst, D., Heald, J. K., Rowland, J. J., Oliver, S. G., and Kell, D. B. 2003. High-throughput classification of yeast mutants for functional genomics using metabolic footprinting. Nat. Biotechnol. 21:692-696.

Allwood, J. W., Ellis, D. I., Heald, J. K., Goodacre, R., and Mur, L. A. 2006. Metabolomic approaches reveal that phosphatidic and phosphatidyl glycerol phospholipids are major discriminatory non-polar metabolites in responses by *Brachypodium distachyon* to challenge by *Magnaporthe grisea*. Plant J. 46:351-368.

Allwood, J. W., Ellis, D. I., and Goodacre, R. 2008. Metabolomic technologies and their application to the study of plants and plant–host interactions. Physiol. Plant. 132:117-135.

Bai, G. H., and Shayner, G. 1996. Variation in *Fusarium graminearum* and cultivar resistance to wheat scab. Plant Dis. 80:975-979.

Baldwin, T. K., Winnenburg, R., Urban, M., Rawlings, C., Koehler, J., and Hammond-Kosack, K. E. 2006. The pathogen–host interactions database (PHI-base) provides insights into generic and novel themes of pathogenicity. Mol. Plant-Microbe Interact. 19:1451-1462.

Baldwin, T. K., Urban, M., Brown, N., and Hammond-Kosack, K. E. 2010. A role for topoisomerase I in *Fusarium graminearum* and *F. culmorum* pathogenesis and sporulation. Mol. Plant-Microbe Interact. 23:566-577.

Bowden, R. L., and Leslie, J. F. 1992. Nitrate-nonutilizing mutants of *Gibberella-zeae* (*Fusarium-graminearum*) and their use in determining vegetative compatibility. Exp. Mycol. 16:308-315.

Brown, D. W., McCormick, S. P., Alexander, N. J., Proctor, R. H., and Desjardins, A. E. 2002. Inactivation of a cytochrome P-450 is a determinant of trichothecene diversity in *Fusarium* spp.. Fungal Genet. Biol. 36:224-233.

Browne, R. A., and Brindle, K. M. 2007. ^{1}H NMR-based metabolite profiling as a potential selection tool for breeding passive resistance against *Fusarium* head blight (FHB) in wheat. Mol. Plant Pathol. 8:401-410.

Choi, Y. H., Tapias, E. C., Kim, H. K., Lefeber, A. W., Erkelens, C., Verhoeven, J. T., Brzin, J., Zel, J., and Verpoorte, R. 2004. Metabolic discrimination of *Catharanthus roseus* leaves infected by phytoplasma using ^{1}H-NMR spectroscopy and multivariate data analysis. Plant Physiol. 135:2398-2410.

Choi, Y. H., Kim, H. K., Linthorst, H. J., Hollander, J. G., Lefeber, A. W., Erkelens, C., Nuzillard, J. M., and Verpoorte, R. 2006. NMR metabolomics to revisit the tobacco mosaic virus infection in *Nicotiana tabacum* leaves. J. Nat. Prod. 69:742-748.

Cuomo, C. A., Guldener, U., Xu, J. R., Trail, F., Turgeon, B. G., Di Pietro, A., Walton, J. D., Ma, L. J., Baker, S. E., Rep, M., Adam, G., Antoniw, J., Baldwin, T., Calvo, S., Chang, Y. L., Decaprio, D., Gale, L. R., Gnerre, S., Goswami, R. S., Hammond-Kosack, K., Harris, L. J., Hilburn, K., Kennell, J. C., Kroken, S., Magnuson, J. K., Mannhaupt, G., Mauceli, E., Mewes, H. W., Mitterbauer, R., Muehlbauer, G., Munsterkotter, M., Nelson, D., O'Donnell, K., Ouellet, T., Qi, W., Quesneville, H., Roncero, M. I., Seong, K. Y., Tetko, I. V., Urban, M., Waalwijk, C., Ward, T. J., Yao, J., Birren, B. W., and Kistler, H. C. 2007. The *Fusarium graminearum* genome reveals a link between localized polymorphism and pathogen specialization. Science 317:1400-1402.

Dawson, W., Jestoi, M., Rizzo, A., Nicholson, P., and Bateman, G. L. 2004. Field evaluation of fungal competitors of *Fusarium culmorum* and *F. graminearum*, causal agents of ear blight of winter wheat, for the control of mycotoxin production in grain. Biocontrol Sci. Technol. 14:783-799.

de Vries, R. P., Flitter, S. J., van de Vondervoort, P. J., Chaveroche, M. K., Fontaine, T., Fillinger, S., Ruijter, G. J., d'Enfert, C., and Visser, J. 2003. Glycerol dehydrogenase, encoded by gldB is essential for osmotolerance in *Aspergillus nidulans*. Mol. Microbiol. 49:131-141.

Forster, J., Famili, I., Fu, P., Palsson, B. Ã., and Nielsen, J. 2003. Genome-scale reconstruction of the *Saccharomyces cerevisiae* metabolic network.

Genome Res. 13:244-253.

Frisvad, J. C., and Samson, R. A. 2004. Polyphasic taxonomy of *Penicillium* subgenus *Penicillium*—a guide to identification of food and air-borne *terverticillate* Penicillia and their mycotoxins. Stud. Mycol. 1-173.

Gaffoor, I., Brown, D. W., Plattner, R., Proctor, R. H., Qi, W., and Trail, F. 2005. Functional analysis of the polyketide synthase genes in the filamentous fungus *Gibberella zeae* (anamorph *Fusarium graminearum*). Eukaryot. Cell 4:1926-1933.

Gale, L. R., Bryant, J. D., Calvo, S., Giese, H., Katan, T., O'Donnell, K., Suga, H., Taga, M., Usgaard, T. R., Ward, T. J., and Kistler, H. C. 2005. Chromosome complement of the fungal plant pathogen *Fusarium graminearum* based on genetic and physical mapping and cytological observations. Genetics 171:985-1001.

Gardiner, D., Kazan, K., and Manners, J. 2009a. Nutrient profiling reveals potent inducers of trichothecene biosynthesis in *Fusarium graminearum*. Fungal Genet. Biol. 46:604-613.

Gardiner, D., Osborne, S., Kazan, K., and Manners, J. 2009b. Low pH regulates the production of deoxynivalenol by *Fusarium graminearum*. Microbiology 155:3149.

Greenhalgh, R., Levandier, D., Adams, W., Miller, J. D., Blackwell, B. A., McAlees, A. J., and Taylor, A. 1986. Production and characterization of deoxynivalenol and other secondary metabolites of *Fusarium culmorum* (CMI 14764, HLX 1503). J. Agric. Food Chem. 34:98-102.

Guldener, U., Seong, K. Y., Boddu, J., Cho, S., Trail, F., Xu, J. R., Adam, G., Mewes, H. W., Muehlbauer, G. J., and Kistler, H. C. 2006. Development of a *Fusarium graminearum* Affymetrix GeneChip for profiling fungal gene expression *in vitro* and *in planta*. Fungal Genet. Biol. 43:316-325.

Hamzehzarghani, H., Kushalappa, A. C., Dion, Y., Rioux, S., Comeau, A., Yaylayan, V., Marshall, W. D., and Mather, D. E. 2005. Metabolic profiling and factor analysis to discriminate quantitative resistance in wheat cultivars against *Fusarium* head blight. Physiol. Mol. Plant Pathol. 66:119-133.

Harris, L. J., Alexander, N. J., Saparno, A., Blackwell, B., McCormick, S. P., Desjardins, A. E., Robert, L. S., Tinker, N., Hattori, J., Piche, C., Schernthaner, J. P., Watson, R., and Ouellet, T. 2007. A novel gene cluster in *Fusarium graminearum* contains a gene that contributes to butenolide synthesis. Fungal Genet. Biol. 44:293-306.

Herrgard, M. J., Swainston, N., Dobson, P., Dunn, W. B., Arga, K. Y., Arvas, M., Buthgen, N., Borger, S., Costenoble, R., Heinemann, M., Hucka, M., Le Novere, N., Li, P., Liebermeister, W., Mo, M. L., Oliveira, A. P., Petranovic, D., Pettifer, S., Simeonidis, E., Smallbone, K., Spasie, I., Weichart, D., Brent, R., Broomhead, D. S., Westerhoff, H. V., Kurdar, B., Penttila, M., Klipp, E., Palsson, B. O., Sauer, U., Oliver, S. G., Mendes, P., Nielsen, J., and Kell, D. B. 2008. A consensus yeast metabolic network reconstruction obtained from a community approach to systems biology. Nat. Biotechnol. 26:1155-1160.

Hestbjerg, H., Nielsen, K. F., Thrane, U., and Elmholt, S. 2002. Production of trichothecenes and other secondary metabolites by *Fusarium culmorum* and *Fusarium equiseti* on common laboratory media and a soil organic matter agar: an ecological interpretation. J. Agric. Food Chem. 50:7593-7599.

Jansen, C., von Wettstein, D., Schafer, W., Kogel, K. H., Felk, A., and Maier, F. J. 2005. Infection patterns in barley and wheat spikes inoculated with wild-type and trichodiene synthase gene disrupted *Fusarium graminearum*. Proc. Nat. Acad. Sci. U.S.A. 102:16892-16897.

Junker, B., Klukas, C., and Schreiber, F. 2006. VANTED: a system for advanced data analysis and visualization in the context of biological networks. BMC Bioinf. 7:109.

Jurgenson, J. E., Bowden, R. L., Zeller, K. A., Leslie, J. F., Alexander, N. J., and Plattner, R. D. 2002. A genetic map of *Gibberella zeae* (*Fusarium graminearum*). Genetics 160:1451-1460.

Kanehisa, M., Araki, M., Goto, S., Hattori, M., Hirakawa, M., Itoh, M., Katayama, T., Kawashima, S., Okuda, S., Tokimatsu, T., and Yamanishi, Y. 2008. KEGG for linking genomes to life and the environment. Nucleic Acid. Res. 36:D480-484.

Keon, J., Antoniw, J., Carzaniga, R., Deller, S., Ward, J., Baker, J., Beale, M., Hammond-Kosack, K., and Rudd, J. 2007. Transcriptional adaptation of *Mycosphaerella graminicola* to programmed cell death (PCD) of its susceptible wheat host. Mol. Plant-Microbe Interact. 20:178-193.

Kimura, M., Tokai, T., O'Donnell, K., Ward, T. J., Fujimura, M., Hamamoto, H., Shibata, T., and Yamaguchi, I. 2003. The trichothecene biosynthesis gene cluster of *Fusarium graminearum* F15 contains a limited number of essential pathway genes and expressed non-essential genes. FEBS (Fed. Eur. Biochem. Soc.) Lett. 539:105-110.

Kouskoumvekaki, I., Yang, Z., Jonsdottir, S.O., Olsson, L., and Panagiotou, G. 2008. Identification of biomarkers for genotyping *Aspergilli* using non-linear methods for clustering and classification. BMC Bioinf. 9:59.

Kubicek, C. P., Hampel, W., and Röhr, M. 1979. Manganese deficiency leads to elevated amino acid pools in citric acid accumulating *Aspergillus niger*. Arch. Microbiol. 123:73-79.

Kumar, S., Punekar, N. S., SatyaNarayan, V., and Venkatesh, K. V. 2000. Metabolic fate of glutamate and evaluation of flux through the 4-aminobutyrate (GABA) shunt in *Aspergillus niger*. Biotechnol. Bioeng. 67:575-584.

Leonard, K. J., and Bushnell, W. R., eds. 2003. Fusarium Head Blight of Wheat and Barley. The American Phytopathological Society, St. Paul, MN, U.S.A.

Li, X., Liu, C., Chakraborty, S., Manners, J., and Kazan, K. 2008. A simple method for the assessment of crown rot disease severity in wheat seedlings inoculated with *Fusarium pseudograminearum*. J. Phytopathol. 156:751-754.

Lowe, R. G., Lord, M., Rybak, K., Trengove, R. D., Oliver, R. P., and Solomon, P. S. 2009. Trehalose biosynthesis is involved in sporulation of *Stagonospora nodorum*. Fungal Genet. Biol. 46:381-389.

Luongo, L., Galli, M., Corazza, L., Meekes, E., De Haas, L., Van der Plas, C. L., and Kohl, J. 2005. Potential of fungal antagonists for biocontrol of *Fusarium* spp. in wheat and maize through competition in crop debris. Biocontrol Sci. Technol. 15:229-242.

Miller, J. D., and Blackwell, B. A. 1986. Biosynthesis of 3-acetyldeoxynivalenol and other metabolites by *Fusarium culmorum* HLK 1503 in a stirred jar fermentor. Can. J. Bot. 64:1-5.

Mitter, V., Zhang, M. C., Liu, C. J., Ghosh, R., Ghosh, M., and Chakraborty, S. 2006. A high-throughput glasshouse bioassay to detect crown rot resistance in wheat germplasm. Plant Pathol. 55:433-441.

Nielsen, K. F., and Smedsgaard, J. 2003. Fungal metabolite screening: database of 474 mycotoxins and fungal metabolites for dereplication by standardized liquid chromatography–UV-mass spectrometry methodology. J. Chromatogr. A 1002:111-136.

O'Donnell, K., Cigelnik, E., and Casper, H. H. 1998. Molecular phylogenetic, morphological, and mycotoxin data support reidentification of the Quorn mycoprotein fungus as *Fusarium venenatum*. Fungal Genet. Biol. 23:57-67.

O'Donnell, K., Ward, T. J., Geiser, D. M., Corby Kistler, H., and Aoki, T. 2004. Genealogical concordance between the mating type locus and seven other nuclear genes supports formal recognition of nine phylogenetically distinct species within the *Fusarium graminearum* clade. Fungal Genet. Biol. 41:600-623.

Oliver, S. G., Winson, M. K., Kell, D. B., and Baganz, F. 1998. Systematic functional analysis of the yeast genome. Trends Biotechnol. 16:373-378.

Panagiotou, G., Christakopoulos, P., and Olsson, L. 2005a. The influence of different cultivation conditions on the metabolome of *Fusarium oxysporum*. J. Biotechnol. 118:304-315.

Panagiotou, G., Christakopoulos, P., and Olsson, L. 2005b. Simultaneous saccharification and fermentation of cellulose by *Fusarium oxysporum* F3—growth characteristics and metabolite profiling. Enzyme Microb. Technol. 36:693-699.

Panagiotou, G., Christakopoulos, P., Villas-Boas, S., and Olsson, L. 2005c. Fermentation performance and intracellular metabolite profiling of *Fusarium oxysporum* cultivated on a glucose–xylose mixture. Enzyme Microb. Technol. 36:100-106.

Panagiotou, G., Villas-Bôas, S.G., Christakopoulos, P., Nielsen, J., and Olsson, L. 2005d. Intracellular metabolite profiling of *Fusarium oxysporum* converting glucose to ethanol. J. Biotechnol. 115:425-434.

Parker, D., Beckmann, M., Zubair, H., Enot, D. P., Caracuel-Rios, Z., Overy, D. P., Snowdon, S., Talbot, N. J., and Draper, J. 2009. Metabolomic analysis reveals a common pattern of metabolic re-programming during invasion of three host plant species by *Magnaporthe grisea*. Plant J. 59:723-737.

Ponts, N., Couedelo, L., Pinson-Gadais, L., Verdal-Bonnin, M. N., Barreau, C., and Richard-Forget, F. 2009. *Fusarium* response to oxidative stress by H_2O_2 is trichothecene chemotype-dependent. FEMS (Fed. Eur. Microbiol. Soc.) Microbiol. Lett. 293:255-262.

Ramirez, M. L., Chulze, S., and Magan, N. 2006. Temperature and water activity effects on growth and temporal deoxynivalenol production by two Argentinean strains of Fusarium graminearum on irradiated wheat grain. Int. J. Food Microbiol. 106:291-296.

Rico, A., and Preston, G. M. 2008. *Pseudomonas syringae pv*. tomato DC3000 uses constitutive and apoplast-induced nutrient assimilation pathways to catabolize nutrients that are abundant in the tomato apoplast. Mol. Plant-Microbe Interact. 21:269-282.

Schauer, N., Semel, Y., Roessner, U., Gur, A., Balbo, I., Carrari, F., Pleban, T., Perez-Melis, A., Bruedigam, C., and Kopka, J. 2006. Comprehensive metabolic profiling and phenotyping of interspecific introgression lines for tomato improvement. Nat. Biotechnol. 24:447.

Schmit, J., and Brody, S. 1975. *Neurospora crassa* conidial germination: role of endogenous amino acid pools. J. Bacteriol. 124:232.

Scott, J. B., and Chakraborty, S. 2006. Multilocus sequence analysis of *Fusarium pseudograminearum* reveals a single phylogenetic species. Mycol. Res. 110:1413-1425.

Smedsgaard, J., and Frisvad, J. C. 1996. Using direct electrospray mass spectrometry in taxonomy and secondary metabolite profiling of crude fungal extracts. J. Microbiol. Methods 25:5-17.

Smedsgaard, J., and Frisvad, J. C. 1997. *Terverticillate penicillia* studied by direct electrospray mass spectrometric profiling of crude extracts. 1. Chemosystematics. Biochem. Syst. Ecol. 25:51-64.

Smedsgaard, J., and Nielsen, J. 2004. Pages 273-286 in: Metabolite Profiling of Fungi and Yeast: From Phenotype to Metabolome by MS and Informatics. Oxford University Press, Edinburgh.

Solomon, P. S., Waters, O. D., Jorgens, C. I., Lowe, R. G., Rechberger, J., Trengove, R. D., and Oliver, R. P. 2006. Mannitol is required for asexual sporulation in the wheat pathogen *Stagonospora nodorum* (glume blotch). Biochem. J. 399:231-239.

Starkey, D. E., Ward, T. J., Aoki, T., Gale, L. R., Kistler, H. C., Geiser, D. M., Suga, H., Toth, B., Varga, J., and O'Donnell, K. 2007. Global molecular surveillance reveals novel Fusarium head blight species and trichothecene toxin diversity. Fungal Genet. Biol. 44:1191-1204.

Strange, R. N., and Smith, H. 1978. Specificity of choline and betaine as stimulants of *Fusarium graminearum* Trans. Br. Mycol. Soc. 70:187-192.

Strange, R. N., Majer, J. R., and Smith, H. 1974. Isolation and identification of choline and betaine as 2 major components in anthers and wheat-germ that stimulate *Fusarium graminearum* in vitro. Physiol. Plant Pathol. 4:277-290.

Tacke, B. K., and Casper, H. H. 1996. Determination of deoxynivalenol in wheat, barley and malt by column cleanup and gas chromatography with electron capture detection. J. AOAC Int. 79:472-475.

Taylor, R. D., Saparno, A., Blackwell, B., Anoop, V., Gleddie, S., Tinker, N., and Harris, L. J. 2008. Proteomic analyses of *Fusarium graminearum* grown under mycotoxin-inducing conditions. Proteomics 8:2256-2265.

Teusink, B., Baganz, F., Westerhoff, H. V., Oliver, S. G., Alistair, J. P. B., and Mick, T. 1998. Metabolic control analysis as a tool in the elucidation of the function of novel genes. Pages 297-336 in: Methods in Microbiology. N. S. Iacobellis, A. Collmer, S. W. Hutcheson, J. W. Mansfield, C. E. Morris, J. Murillo, N. W. Schaad, D. E. Stead, G. Surico, and M. Ullrich, eds. Kluwer Academic Academic Press, Dordrecht, The Netherlands.

Trail, F., and Common, R. 2000. Perithecial development by *Gibberella zeae:* a light microscopy study. Mycologia 92:130-138.

Trinci, A. P. 1994. The 1994 Marjory Stephenson Prize Lecture. Evolution of the Quorn myco-protein fungus, *Fusarium graminearum* A3/5. Microbiology 140:2181-2188.

Urban, M., Daniels, S., Mott, E., and Hammond-Kosack, K. 2002. *Arabidopsis* is susceptible to the cereal ear blight fungal pathogens *Fusarium graminearum* and *Fusarium culmorum*. Plant J. 32:961-973.

Urban, M., Mott, E., Farley, T., and Hammond-Kosack, K. 2003. The *Fusarium graminearum MAP1* gene is essential for pathogenicity and development of perithecia. Mol. Plant Pathol. 4:347-359.

Ward, J. L., Harris, C., Lewis, J., and Beale, M. H. 2003. Assessment of ^{1}H NMR spectroscopy and multivariate analysis as a technique for metabolite fingerprinting of *Arabidopsis thaliana*. Phytochemistry 62:949-957.

Ward, J. L., Forcat, S., Beckmann, M., Bennett, M., Miller, S. J., Baker, J. M., Hawkins, N. D., Vermeer, C. P., Lu, C., Lin, W., Truman, W. M., Beale, M. H., Draper, J., Mansfield, J. W., and Grant, M. 2010. The metabolic transition during disease following infection of *Arabidopsis thaliana* by *Pseudomonas syringae* pv. *tomato*. Plant J. 63:443-457.

Ward, T., Clear, R., Rooney, A., O'Donnell, K., Gaba, D., Patrick, S., Starkey, D., Gilbert, J., Geiser, D., and Nowicki, T. 2008. An adaptive evolutionary shift in *Fusarium* head blight pathogen populations is driving the rapid spread of more toxigenic *Fusarium graminearum* in North America. Fungal Genet. Biol. 45:473-484.

Wiebe, M. G. 2004. Quorn(TM) Myco-protein—overview of a successful fungal product. Mycologist 18:17-20.

Wilson, R. A., Jenkinson, J. M., Gibson, R. P., Littlechild, J. A., Wang, Z. Y., and Talbot, N. J. 2007. Tps1 regulates the pentose phosphate pathway, nitrogen metabolism and fungal virulence. EMBO (Eur. Mol. Biol. Organ.) J. 26:3673-3685.

Winnenburg, R., Baldwin, T. K., Urban, M., Rawlings, C., Kohler, J., and Hammond-Kosack, K. E. 2006. PHI-base: a new database for pathogen host interactions. Nucleic Acids Res. 34:D459-464.

Winnenburg, R., Urban, M., Beacham, A., Baldwin, T. K., Holland, S., Lindeberg, M., Hansen, H., Rawlings, C., Hammond-Kosack, K. E., and Kohler, J. 2008. PHI-base update: additions to the pathogen host interaction database. Nucleic Acids Res. 36:D572-576.

Wold, S., Antti, H., Lindgren, F., and Öhman, J. 1998. Orthogonal signal correction of near-infrared spectra. Chemom. Intell. Lab. Syst. 44:175-185.

AUTHOR-RECOMMENDED INTERNET RESOURCE

Bruker Biospin website: www.bruker-biospin.com